

*Chapter 5***SYNTHESIS AND PROPERTIES OF ND-DOPED
Bi₄Ti₃O₁₂ USING THE SOFT COMBUSTION
TECHNIQUE**

*A. Umar Al-Amani, S. Sreekantan, M. N. Ahmad Fauzi
and K. A. Razak**

School of Materials and Mineral Resources Engineering,
Universiti Sains Malaysia, 14300 Nibong Tebal, Penang, Malaysia

ABSTRACT

Nd-doped Bi₄Ti₃O₁₂ ceramics, Bi_{4-x}Nd_xTi₃O₁₂ (BNT, x = 0, 0.25, 0.50, 0.75 and 1), were prepared using a soft combustion technique and their phase, structure, thermal behavior, grain morphology, dielectric and ferroelectric properties were investigated. The single phase of BIT was successfully obtained at different synthesis temperature, just after combustion took place at 450°C. The thermal analysis confirmed the phase formation with corresponding temperature. The single phase of BIT was also obtained with different Nd doping. It was also shown that Nd doping had a significance change in Raman and Fourier Transform Infrared spectroscopy (FTIR) spectra. Further increase the sintering temperature at 900°C did not show the presence of secondary phase in X-ray diffraction (XRD) pattern. The average grain length and width decreased with Nd content. The Curie temperature of BNT also reduced to 434°C. The remanent polarization, 2P_r and coercive field, 2E_c of BNT were higher than BIT, whereby the BNT 075 ceramics exhibited the maximum 2P_r and 2E_c values of about 18.4 μC/cm² and 100.6 kV/cm, respectively.

Keywords: Bismuth titanate; Doping; Soft combustion; Lanthanide.

* khairunsak@eng.usm.my

INTRODUCTION

Ion doping technique is a preferable way to enhance the electrical properties of many ceramic materials to date. For instance, bismuth titanate ($\text{Bi}_4\text{Ti}_3\text{O}_{12}$ or BIT) has been reported to exhibit low remanent polarization ($2P_r < 10 \mu\text{C}/\text{cm}^2$), high leakage current, low fatigue resistant, high dielectric loss and high electrical conductivity which limit its application in a non-volatile ferroelectric random access memory technology (NvFRAM) [1-3]. In order to solve these issues, many researchers suggested that ferroelectric properties of BIT can be improved by tuning its composition using ion doping technique. Park et al. [4] found that La^{3+} ion successfully doped in BIT film which the film had enhanced P_r ($16 - 20 \mu\text{C}/\text{cm}^2$), low leakage current ($10^{-7} \text{ A}/\text{cm}^2$ at 5V) and good fatigue resistant (3×10^{10} switching cycles). Kojima et al. [5] reported that the P_r up to $25 \mu\text{C}/\text{cm}^2$ with fatigue free after 2×10^{10} cycles could be achieved when Nd was partially doped in BIT thin film. Chon et al. [6] reported that the $\text{Bi}_{3.15}\text{Sm}_{0.85}\text{Ti}_3\text{O}_{12}$ thin film has high P_r and good fatigue endurance to reach about $29.5 \mu\text{C}/\text{cm}^2$ and 4.5×10^{10} switching cycles. However, the increase in these values was strongly dependent on several things such as the annealing temperature and type of annealing, substrate type, bottom electrode, grain orientation, film thickness etc.

Lanthanide doped BIT has been prepared using the conventional solid-state reaction [7-14], sol-gel method [15-25], hydrolysis method [26, 27], polymeric precursor method [28, 29], chemical solution deposition (CSD) [30-33], metal organic solution decomposition (MOD) [34-39], pulsed laser deposition (PLD) [40], and metalorganic chemical vapor deposition (MOCVD) [41]. Each method has own merits and drawbacks. Conventionally prepared powder often uses high calcination temperature with repeated grinding in its process which then produces hard powder and high agglomeration. As an alternative, wet chemical synthesis is beneficial to reduce the calcination temperature and improve the reactivity and homogeneity of the composition. For deposition process of thin films, the PVD, CVD, MOCVD and rf sputtering are costly and the parameter settings are also complex. Sol-gel method is the simplest method to produce thin films. Sol-gel method also offers several advantages including pre- and post-deposition at low temperature, easier compositional control and better uniformity of the films, economical compared to CVD and PVD techniques [3].

To the best of authors' knowledge, very least works on soft combustion technique have been reported. Previously, this technique has been used extensively to prepare a large number of technologically useful oxide materials such as refractories, magnetic, semiconductors, dielectric, catalyst, sensors, phosphors, etc. and none oxide materials such as carbides, nitrides, borides and silicides [42, 43]. This approach is convenient, requires simple experimental set up and save time as well as requires low energy consumption [44]. This is because this technique is characterized by self-sustaining solution combustion synthesis in which the exothermicity of the redox chemical reaction is used to produce the useful materials [45]. Recently, our group used glycine to produce praseodymium-doped bismuth potassium titanate and praseodymium-doped bismuth sodium titanate [46, 47]. There also a study on praseodymium-doped bismuth titanate, however, the fuel agent was not introduced in synthesis process [48]. In the present study, Nd was partially doped in BIT using a novelty low combustion synthesis temperature without calcination process. The prepared samples

were investigated in terms of phase formation, thermal behavior, structure, grain morphology, dielectric and ferroelectric properties.

EXPERIMENTAL PROCEDURE

Nd-doped BIT ($\text{Bi}_{4-x}\text{Nd}_x\text{Ti}_3\text{O}_{12}$) were prepared according to the Nd content $x = 0, 0.25, 0.50, 0.75$ and 1 , the samples are denoted as BIT, BNT025, BNT050, BNT075 and BNT100, respectively. Firstly, bismuth nitrate ($\text{Bi}(\text{NO}_3)_3 \cdot 5\text{H}_2\text{O}$, Sigma-Aldrich, 98 %) was dissolved at 40°C in distilled water. Separately, neodymium nitrate ($\text{Nd}(\text{NO}_3)_3 \cdot 6\text{H}_2\text{O}$, Sigma-Aldrich, 99.9 %) was dissolved in distilled water and citric acid ($\text{C}_6\text{H}_8\text{O}_7$, Sigma-Aldrich, 99.5 %) was used as a fuel agent. The neodymium solution together with citric aqueous were added into the bismuth solution with continuous stirring. The titanium solution was prepared from titanium isopropoxide ($\text{Ti}[\text{OCH}(\text{CH}_3)_2]_4$, Aldrich Chemistry, 97 %) which was initially dissolved in 2-methoxyethanol (Sigma-Aldrich, ≥ 99). Finally, the titanium solution was slowly added into the bismuth neodymium solution to obtain the precursor solution. This solution was adjusted to pH7 with NH_4OH (29 % solution). The prepared solution was stirred at 60°C for additional 24 h to obtain a homogeneous solution. After that, the temperature was increased to 80°C to form a dried precipitates. The precipitates were gently crushed using an agate mortar pestle. The crushed powder was heated on a hot plate attached with thermocouple for the soft combustion process to take place, and the temperature was recorded $\sim 450^\circ\text{C}$. The reaction lasted less than 5 min and produced yellowish and greenish powders for BIT and BNT powders, respectively.

Thermal behavior of the dried powder was investigated using Thermogravimetry-Differential Thermal Analysis, TG-DTA (Linesis). Phase identification was investigated by X-Ray Diffraction with $\text{Cu-K}\alpha$ radiation, X-ray diffraction (XRD) (Bruker D8 Advanced). Raman spectrometer (Horiba Jobin-Yvon HR800UV) and FTIR spectrophotometer (Perkin Elmer) were used to investigate the phonon mode and adsorption band, respectively. The microstructure of the prepared samples was examined using a field emission scanning electron microscopy, FESEM [Zeiss Supra 55VP PGT/HKL]. To investigate the dielectric and ferroelectric properties, the sintered pellet was coated with silver conductive paint and fired at 700°C for 15 min. The capacitance and loss tangent were measured using an Impedance analyzer (Hewlett Packard 4192A LF). The ferroelectric P-E hysteresis loop was investigated using Sawyer-Tower circuit.

RESULT AND DISCUSSION

Figure 1 shows the XRD patterns of the BIT powder prepared at different synthesis temperatures. The XRD patterns were compared with standard BIT data (JCPDS 73-2181). It was found that a stable phase BIT with layered perovskite structure could be obtained at temperatures between 40 and 60°C . Additionally, the stability of phase formation was also achieved in calcined powder at 500°C . This indicates that the synthesis temperature is sufficient to obtain the single phase of BIT without further calcination process.

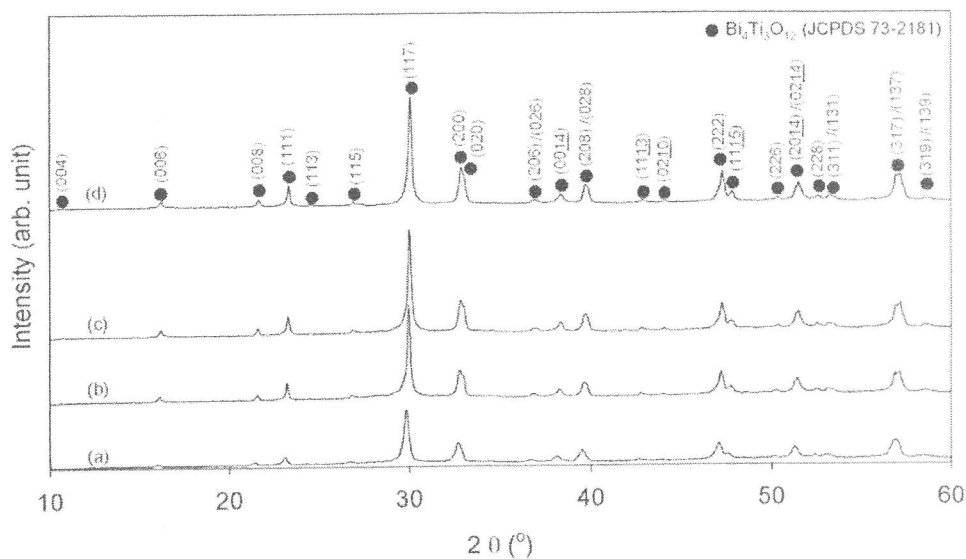


Figure 1. XRD patterns of BIT powder at different synthesis temperatures: (a) 40°C, (b) 50°C, (c) 60°C and (d) calcination at 500°C for (c) samples.

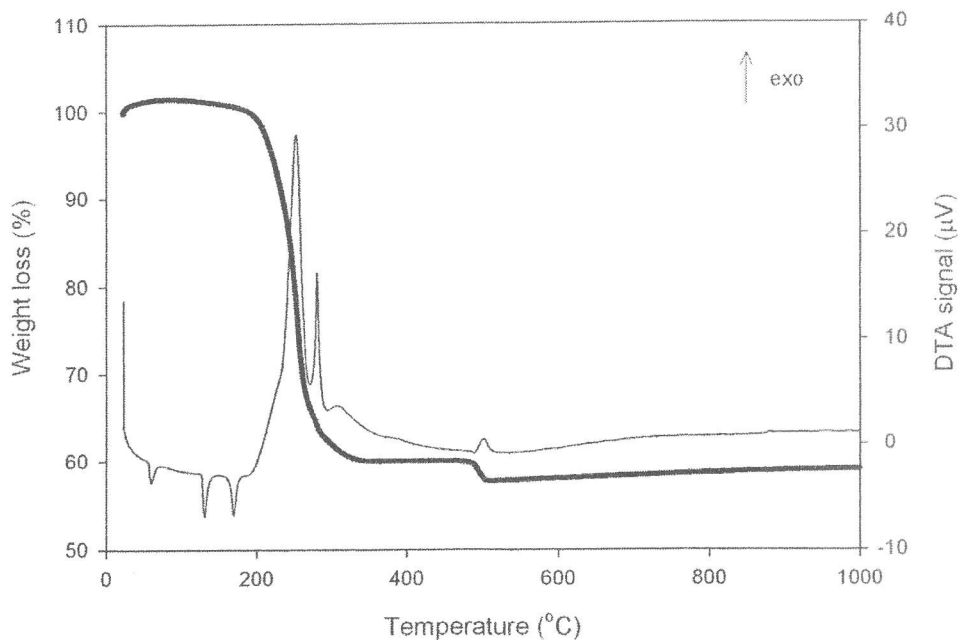


Figure 2. TG and DTA of BIT powder derived from 60°C.

Figure 2 shows the TG and DTA of BIT powder derived at 60°C. As shown in Figure 2, the TG curve can be divided into two distinct stages. The first weight loss took place at temperature range of 100 - 355°C and second weight loss at temperature range of 480 - 505°C. Above 505°C, the reaction was completed as indicated by linear curve. The total weight loss of about 42.4 % was obtained for BIT powder. The DTA curve showed the

endothermic peaks at approximate 60, 130 and 170°C, while exothermic peak at approximate 252, 280, 307 and 501°C. The corresponding endothermic peaks could be ascribed to the vaporization of residual water and organic substances, which correspond to a small weight loss. The exothermic peaks between 183 and 347°C could be explained by decomposition of the nitrate and combustion/pyrolysis of the Bi-Ti organic chelating agent [49]. This is supported by massive weight loss of about 39.8% on the TG curve. A small exothermic peak at final weight loss could be due to phase transition from amorphous oxides to BIT compound.

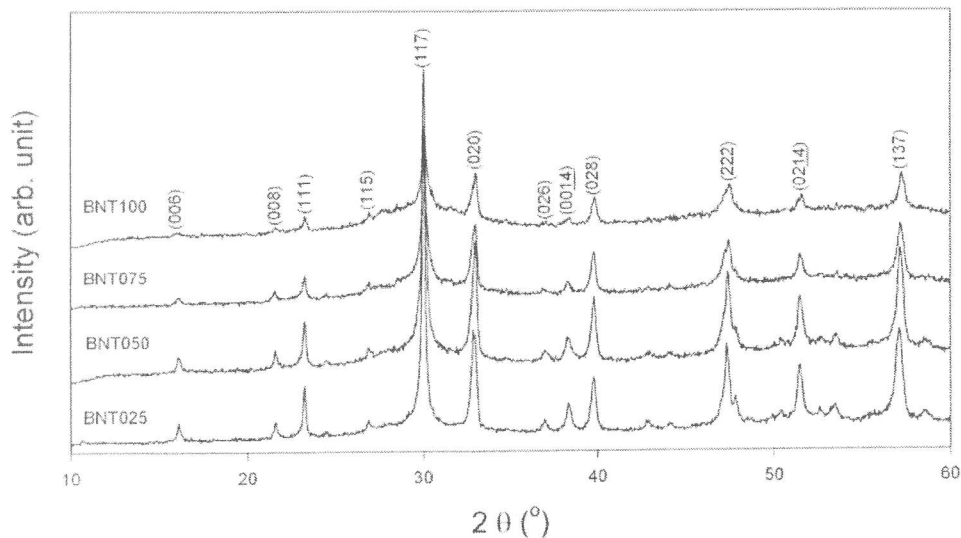


Figure 3. XRD patterns of BNT powders.

Figure 3 shows the XRD patterns of BNT powders with various contents. The diffraction peaks are indexed using the standard data of BIT phase (JCPDS 73-2181). It was found that a single phase was obtained for all compositions that indicates Nd^{3+} ions were fully dissolved in the BIT solid solution. Additionally, the intensity of diffraction peaks were found to decrease and to have a broaden peak with Nd doping. Broadening of the peak indicates the decrease of crystallite size [47].

Figure 4 shows the Raman spectra of BIT, BNT025 and BNT075 at room temperature from 100 to 2000 cm^{-1} . The BIT exhibits a sharp and narrow peak with high intensity in five Raman modes at 267, 322, 537, 615 and 848 cm^{-1} .

These modes characteristic changed with Nd content, which corresponded to the decrease in intensity and the increase in peak width. The peaks became broader and only showed three Raman modes as shown in BNT075. The interaction of internal mode of TiO_6 octahedra appeared above 200 cm^{-1} due to large intragroup binding energy in the octahedra and the much smaller mass of Ti^{4+} ions [50, 51].

In the case of BIT, the mode at 267 cm^{-1} ascribed from the torsional bending of TiO_6 and those at 615 and 848 cm^{-1} assigned to the stretching vibration. The mode at 322 cm^{-1} was from a combination of the stretching and bending vibrations. The mode at 537 cm^{-1} was ascribed to the O-Ti-O stretching vibrations.

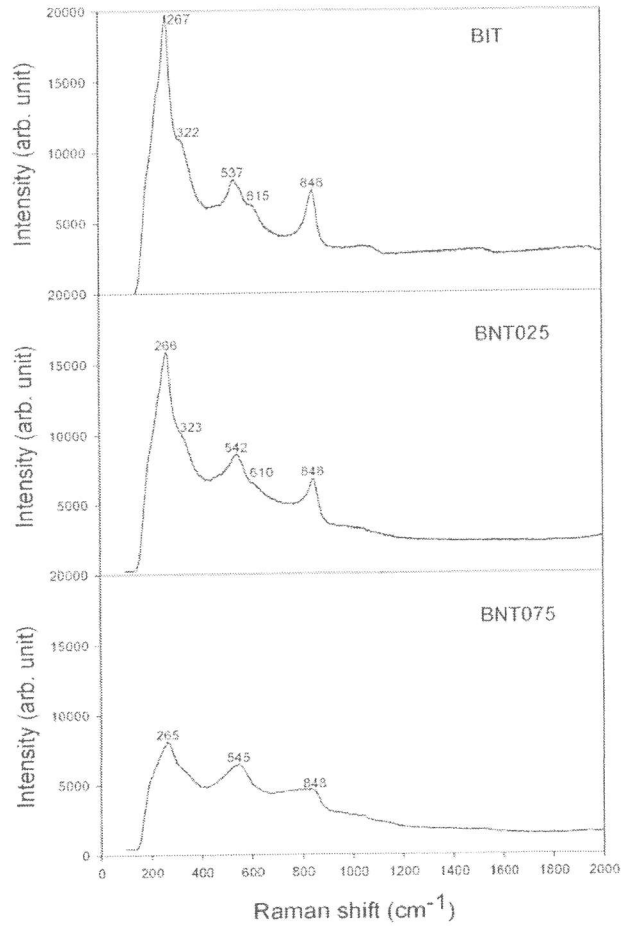


Figure 4. Raman spectrum of BIT, BNT025 and BNT075 at room temperature.

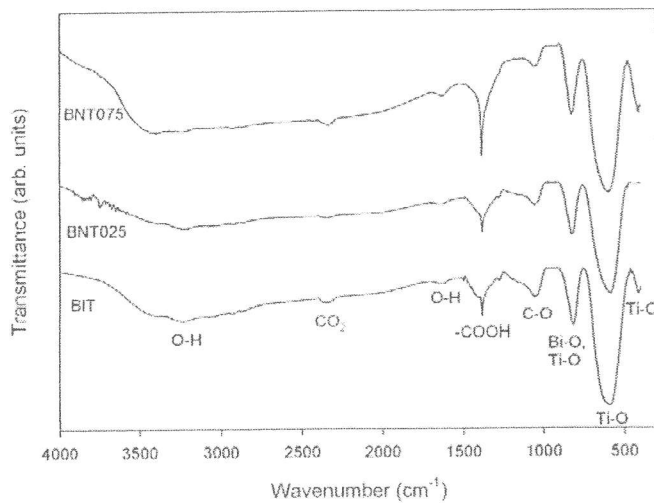


Figure 5. FTIR spectra of BIT, BNT025 and BNT075 at room temperature.

The FTIR spectra of BIT, BNT025 and BNT075 are shown in Figure 5. Three adsorption bands appeared at 815, 587 and 418 cm⁻¹ were ascribed the perovskite-layered structure of BIT. The band at 815 and 587 cm⁻¹ belong to the Ti-O stretching vibrations while the peak around 418 cm⁻¹ corresponded to the Ti-O bending vibration. The broad peak above 3000 cm⁻¹ and a small peak at 1645 cm⁻¹ were attributed to the stretching vibration of O-H groups and the bending vibrations of absorbed molecular water and 2-methoxyethanol, respectively. The weak peak at 2365 cm⁻¹ belonged to the stretching vibrations of CO₂, while the stretching vibration for carboxylic group (-COOH) was indicated by the presence of band at 1385 cm⁻¹. The bending vibrations of C-O were detected at 1052 cm⁻¹, indicating that a few organic groups were absorbed on the surface of the powders.

Figure 6 shows the XRD patterns of BIT and BNT ceramics sintered at 900°C for 3 h. Regardless of the Nd contents, all the ceramic samples were pure phase with no secondary phase. This indicates that the stability of BIT phase with Nd doping at high sintering temperature. Additionally, the intensity of diffraction peaks was found to decrease with increasing Nd content. It also suggested that Nd doping has a significance effect on the crystallite size and lattice parameter of BIT.

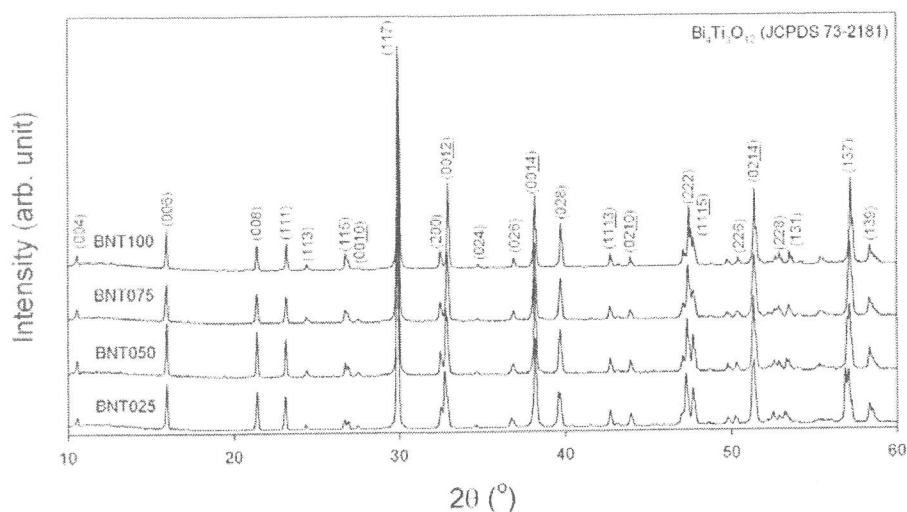


Figure 6. XRD patterns of BNT ceramics sintered at 900°C for 3 h.

Table 1. Average grain length and width of BIT and BNT ceramics

Compositions	Average length (μm)	Average width (μm)
BIT	10.66	1.57
BNT025	8.14	1.33
BNT050	6.88	1.10
BNT075	6.37	0.90
BNT100	5.19	0.78

Figure 7 shows the SEM micrographs of BIT and BNT ceramics. All the ceramics with different Nd content exhibited rod-like grains. The grain size of BIT was larger than that of

BNT, both in terms of grain length and width. Additionally, the grain size of BNT ceramics decreased with increasing Nd content. The calculated average grain length and thickness is presented in Table 1. This indicates that Nd could act as grain growth inhibitor.

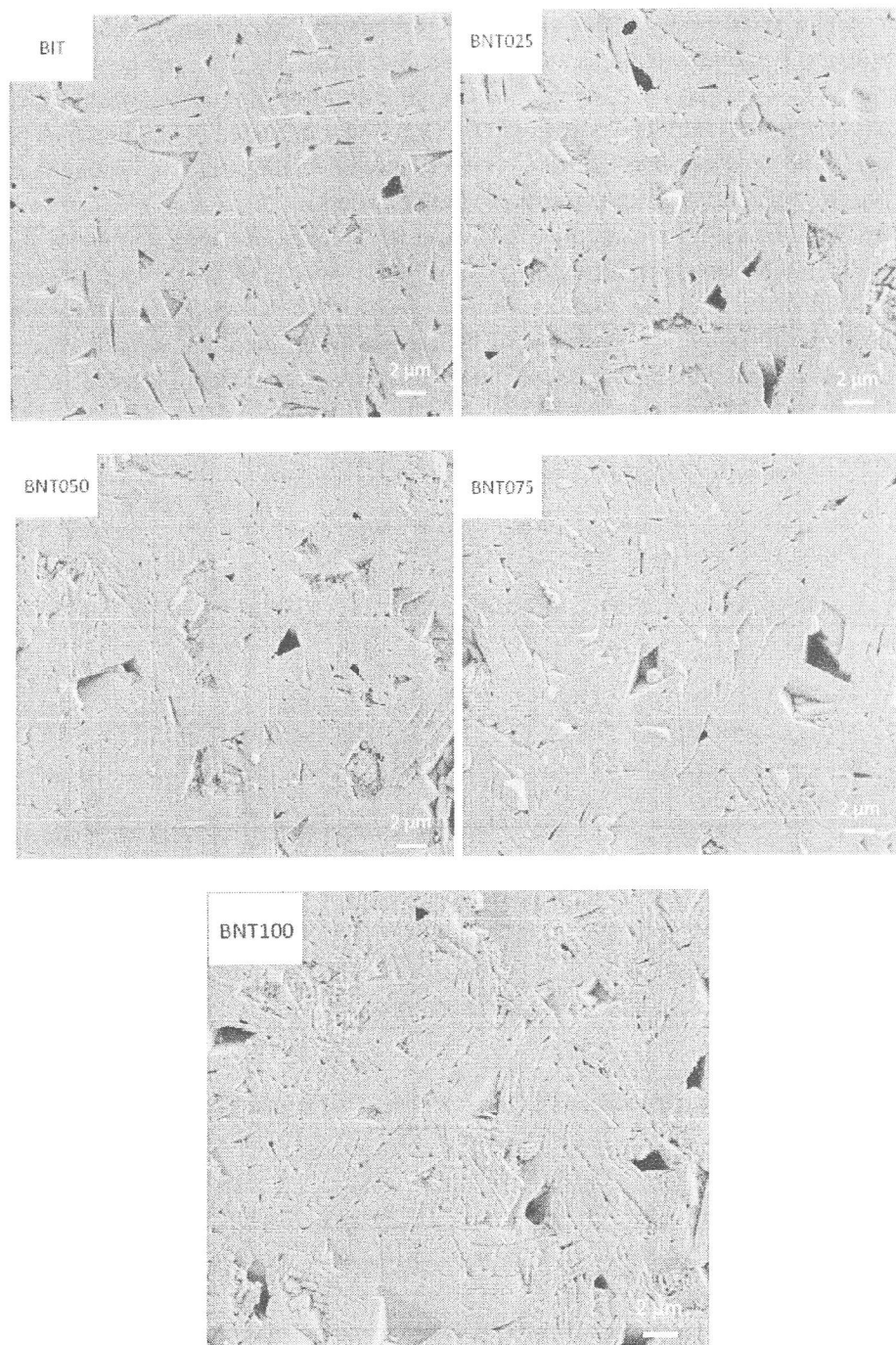


Figure 7. SEM micrographs of BIT and BNT ceramics.

Figure 8 shows the temperature dependence of the dielectric properties of BIT and BNT075 ceramics, measured at 1 MHz. With increasing temperature, the dielectric constant increases and has a maximum peak at the Curie temperature T_c . The T_c of BIT is 675°C . On the other hand, BNT075 has lower T_c value of 434°C . This indicates that the T_c decreased with Nd doping. Additionally, the dielectric peak broadens with Nd doping, indicating the diffusing of the ferro-paraelectric phase transition. The partial substitution of Nd for Bi in BNT significantly reduced the loss tangent as shown in Figure 8.

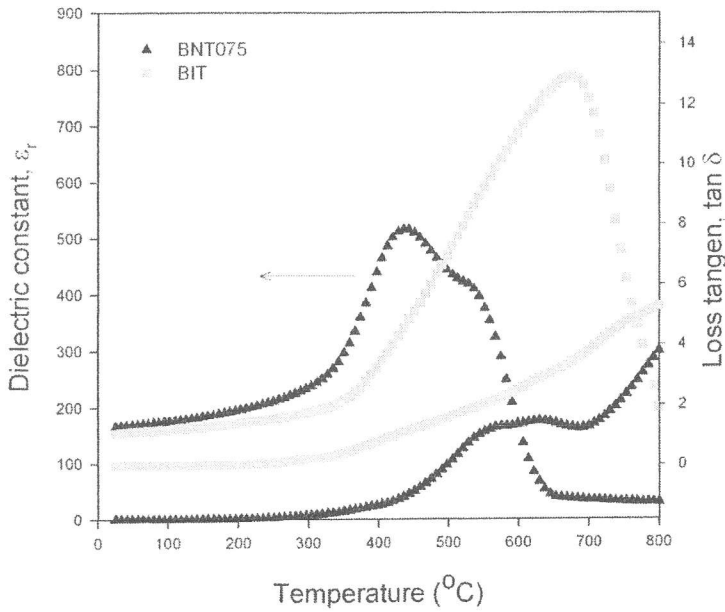


Figure 8. Dielectric properties of BIT and BNT075 as a function of temperature.

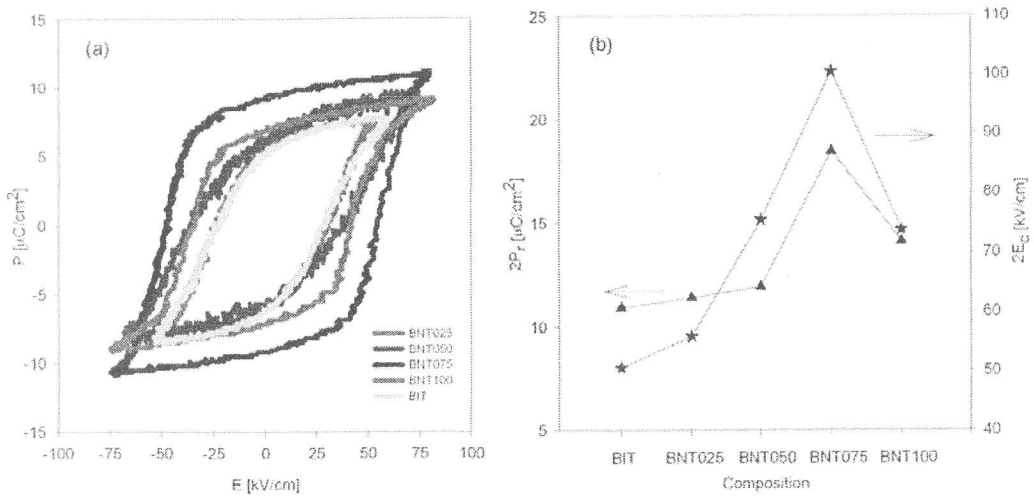


Figure 9. Ferroelectric hysteresis loops of BIT and BNT ceramics.

The ferroelectric hysteresis loops of BIT and BNT ceramic measured at the applied field of 75 kV/cm are illustrated in Figure 9(a). The remanent polarization, $2P_r$ and coercive field, $2E_c$ were plotted in Figure 9(b). As shown in both figures, the $2P_r$ and $2E_c$ are strongly dependent on Nd content. The $2P_r$ and $2E_c$ increase from 0 to 0.75 and decrease beyond that. Then, the BNT075 ceramics shows the maximum $2P_r$ and $2E_c$ values of $18.4 \mu\text{C}/\text{cm}^2$ and $100.6 \text{ kV}/\text{cm}$, respectively. These values are higher than that of BIT ceramic of $10.9 \mu\text{C}/\text{cm}^2$ and $50.6 \text{ kV}/\text{cm}$. This indicates that Nd doping improved ferroelectricity.

CONCLUSION

The single phase of BIT was obtained at different synthesis temperatures using the soft combustion technique. Nd-doped $\text{Bi}_4\text{Ti}_3\text{O}_{12}$ was successfully investigated in terms of phase formation, structure, thermal behavior, grain morphology, dielectric and ferroelectric properties. Thermal analysis showed the reaction was highly exothermic and completed at 500°C . The influence of Nd doping on Raman mode and FTIR spectra was clearly observed in both analysis. Additionally, the grain size both the length and width exhibited in small size at higher Nd content. The maximum dielectric peak was found to be broaden and to have a reduced Curie temperature, T_c with Nd doping. The ferroelectric properties was also improved with Nd content.

ACKNOWLEDGMENT

The authors appreciate the technical support provided by School of Materials and Mineral Resources Engineering, Universiti Sains Malaysia, Prof. Uematsu Keizo and Assoc. Prof. Tanaka Satoshi of Nagaoka University of Technology, Japan. This research was supported by USM-RU grant 1001/PBahan/8042018 and 1001/PBahan/811069.

REFERENCES

- [1] Sedlar, M., Sayer, M., *Ceramics International*, 22, 3, 1996.
- [2] Yamaguchi, M., Kawanabe, K., Nagatomo, T., Omoto, O., *Materials Science and Engineering B*, 41, 1, 1996.
- [3] Madeswaran, S., Giridharan, N. V., Jayavel, R., *Materials Chemistry and Physics*, 80, 1, 2003.
- [4] Park, B. H., Kang, B. S., Bu, S. D., Noh, T. W., Lee, J., Jo, W., *Nature*, 401, 6754, 1999.
- [5] Kojima, T., Sakai, T., Watanabe, T., Funakubo, H., Saito, K., Osada, M., *Applied Physics Letters*, 80, 15, 2002.
- [6] Chon, U., Kim, K. B., Jang, H. M., Yi, G. C., *Applied Physics Letters*, 79, 2001.
- [7] Yao, Y. Y., Song, C. H., Bao, P., Su, D., Lu, X. M., Zhu, J. S., Wang, Y. N., *Journal of Applied Physics*, 95, 6, 2004.

- [8] Kim, J. S., Lee, S. Y., Lee, H. J., Ahn, C. W., Kim, I. W., Jang, M. S., *Journal of Electroceramics*, 21, 1-4 SPEC. ISS., 2008.
- [9] Chen, M., Liu, Z. L., Wang, Y., Wang, C. C., Yang, X. S., Yao, K. L., *Physica Status Solidi (A) Applied Research*, 200, 2, 2003.
- [10] Chen, M., Liu, Z. L., Wang, Y., Wang, C. C., Yang, X. S., Yao, K. L., *Physica B: Condensed Matter*, 352, 1-4, 2004.
- [11] Mao, X. Y., Mao, F. W., Chen, X. B., *Integrated Ferroelectrics*, 79, 1, 2006.
- [12] Tang, Q. Y., Kan, Y. M., Li, Y. G., Zhang, G. J., Wang, P. L., *Solid State Communications*, 142, 1-2, 2007.
- [13] Wang, W., Zhu, J., Mao, X. Y., Chen, X. B., *Journal of Physics D: Applied Physics*, 39, 2, 2006.
- [14] Pineda-Flores, J. L., Chavira, E., Reyes-Gasga, J., González, A. M., Huanosta-Tera, A., *Journal of the European Ceramic Society*, 23, 6, 2003.
- [15] Chen, X. Q., Qi, H. Y., Qi, Y. J., Lu, C. J., *Physics Letters, Section A: General, Atomic and Solid State Physics*, 346, 1-3, 2005.
- [16] Cui, L., Hu, Y. J., *Physica B: Condensed Matter*, 404, 1, 2009.
- [17] Fan, S., Zhang, F., Wang, P., Ren, Y., *Journal of Rare Earths*, 26, 4, 2008.
- [18] Kim, J., Kim, J. K., Heo, S., Lee, H. S., *Thin Solid Films*, 503, 1-2, 2006.
- [19] Ke, H., Wang, W., Chen, L., Xu, J., Jia, D., Lu, Z., Zhou, Y., *Journal of Sol-Gel Science and Technology*, 53, 1,
- [20] Guo, D. Y., Li, M. Y., Liu, J., Fu, L., Wang, J., Yu, B. F., Yang, B., *Materials Science and Engineering B: Solid-State Materials for Advanced Technology*, 142, 2-3, 2007.
- [21] Bae, J. C., Kim, S. S., Choi, E. K., Song, T. K., Kim, W. J., Lee, Y. I., *Thin Solid Films*, 472, 1-2, 2005.
- [22] Tajiri, T., Sumitani, K., Haruki, R., Kohno, A., *IEEE Transactions on Ultrasonics, Ferroelectrics, and Frequency Control*, 54, 12, 2007.
- [23] Lu, C. J., Qiao, Y., Qi, Y. J., Chen, X. Q., Zhu, J. S., *Applied Physics Letters*, 87, 22, 2005.
- [24] Tomar, M. S., Melgarejo, R. E., Singh, S. P., *Microelectronics Journal*, 36, 3-6, 2005.
- [25] Bae, J. C., Kim, S. S., Park, M. H., Jang, K. W., Lee, Y. I., Song, J. S., *Journal of Crystal Growth*, 268, 1-2, 2004.
- [26] Kan, Y. M., Zhang, G. J., Wang, P. L., Cheng, Y. B., *Journal of the European Ceramic Society*, 28, 8, 2008.
- [27] Kan, Y., Jin, X., Zhang, G., Wang, P., Cheng, Y. B., Yan, D., *Journal of Materials Chemistry*, 14, 24, 2004.
- [28] Simões, A. Z., Quinelato, C., Ries, A., Stojanovic, B. D., Longo, E., Varela, J. A., *Materials Chemistry and Physics*, 98, 2-3, 2006.
- [29] Simões, A. Z., Stojanovic, B. D., Zaghete, M. A., Riccardi, C. S., Ries, A., Moura, F., Longo, E., Varela, J. A., *Integrated Ferroelectrics*, 60, 2004.
- [30] Yang, B., Zhang, D. M., Zhou, B., Huang, L. H., Zheng, C. D., Wu, Y. Y., Guo, D. Y., Yu, J., *Journal of Crystal Growth*, 310, 21, 2008.
- [31] Chen, Y. C., Hsiung, C. P., Chen, C. Y., Gan, J. Y., Sun, Y. M., Lin, C. P., *Thin Solid Films*, 513, 1-2, 2006.
- [32] Chen, Y. C., Sun, Y. M., Lin, C. P., Gan, J. Y., *Journal of Crystal Growth*, 268, 1-2, 2004.
- [33] Hu, X., Garg, A., Barber, Z. H., *Thin Solid Films*, 484, 1-2, 2005.

- [34] Giridharan, N., Supriya, S., *Thin Solid Films*, 516, 16, 2008.
- [35] He, H., Huang, J., Cao, L., Wang, L., *Microelectronic Engineering*, 85, 3, 2008.
- [36] Liu, W. L., Xia, H. R., Han, H., Wang, X. Q., *Materials Research Bulletin*, 39, 9, 2004.
- [37] Liu, W. L., Xia, H. R., Han, H., Wang, X. Q., *Journal of Crystal Growth*, 264, 1-3, 2004.
- [38] Liu, W. L., Xia, H. R., Han, H., Wang, X. Q., *Materials Letters*, 58, 24, 2004.
- [39] Liu, W. L., Xia, H. R., Han, H., Wang, X. Q., *Journal of Solid State Chemistry*, 177, 9, 2004.
- [40] Zhang, S. T., Zhang, X. J., Cheng, H. W., Chen, Y. F., Liu, Z. G., Ming, N. B., Hu, X. B., Wang, J. Y., *Applied Physics Letters*, 83, 21, 2003.
- [41] Kojima, T., Sakai, T., Watanabe, T., Funakubo, H., Saito, K., Osada, M., *Applied Physics Letters*, 80, 2002.
- [42] Patil, K. C., Aruna, S. T., Mimani, T., *Current Opinion in Solid State and Materials Science*, 6, 6, 2002.
- [43] Luo, S., Tang, Z., Yao, W., Zhang, Z., *Microelectronic Engineering*, 66, 1-4, 2003.
- [44] Berger, D., Matei, C., Papa, F., Voicu, G., Fruth, V., *Progress in Solid State Chemistry*, 35, 2-4 SPEC. ISS., 2007.
- [45] Patil, K. C., *Bulletin of Materials Science*, 16, 6, 1993.
- [46] Ng, C. Y., Razak, K. A., *Journal of Alloys and Compounds*, 509, 3,
- [47] Razak, K. A., Yip, C. J., Sreekantan, S., *Journal of Alloys and Compounds*, 509, 6,
- [48] Goh, P. Y., Razak, K. A., Sreekantan, S., *Journal of Alloys and Compounds*, 475, 1-2, 2009.
- [49] Du, X., Xu, Y., Ma, H., Wang, J., Li, X., *Journal of the American Ceramic Society*, 90, 5, 2007.
- [50] Kojima, S., *Ferroelectrics*, 239, 1-4, 2000.
- [51] Zhu, J., Chen, X. B., He, J. H., Shen, J. C., *Journal of Solid State Chemistry*, 178, 9, 2005.